Talanta 119 (2014) 485–491

Contents lists available at ScienceDirect

Talanta

journal homepage: www.elsevier.com/locate/talanta

# Hybrid organic–inorganic monolithic enzymatic reactor with SBA-15 nanoparticles incorporated

Zhaodi Zhang [a,b,1], Lingyi Zhang [a,*,1], Chenggong Zhang [b], Weibing Zhang [a]

[a] Shanghai Key Laboratory of Functional Materials Chemistry, East China University of Science and Technology, Shanghai 200237, PR China
[b] Shanghai Key Laboratory of Crime Scene Evidence, Institute of Forensic Science, Shanghai Public Security Bureau, Shanghai, PR China

ARTICLE INFO

*Article history:*
Received 31 July 2013
Received in revised form
11 November 2013
Accepted 13 November 2013
Available online 27 November 2013

*Keywords:*
Enzymatic reactor
SBA-15 nanoparticles
Hybrid organic–inorganic monolith
Trypsin

ABSTRACT

A novel enzymatic reactor was prepared by incorporating SBA-15 nanoparticles into hybrid organic–inorganic monolith and immobilizing trypsin with glutaraldehyde as bridging reagent. Preparation and operation conditions including nanoparticles percentage and residence time were optimized to improve the digestion efficiency. The digestion products were characterized by Matrix Assisted Laser Desorption Ionization Time of Flight Mass Spectrometry (MALDI-TOF-MS) with sequence coverage of 50%, 93% and 71% for bovine serum albumin, myoglobin and cytochrome C, while consuming only about 19 s in dynamic mode. Compared with enzymatic reactor without nanoparticles incorporated, the enzymatic reactor with SBA-15 nanoparticles embedded achieved higher digestion efficiency by introducing more trypsin, which was originated from combination of SBA-15 nanoparticles and hybrid organic–inorganic monolith.



## 1. Introduction

Nowadays, the bottom-up strategy based proteomic study has drawn high attention, in which protein extracts are digested with an enzyme such as trypsin, and the resulting peptides are separated by liquid chromatography and identified by mass spectrometry [1,2]. Obviously, rapid and complete proteolysis is indispensable to this approach [3]. The conventional proteolysis performed in solution suffers from disadvantages of time-consuming and incomplete digestion for low-abundance proteins, which severely restrict the analytical throughput and accuracy of protein identification and characterization [4]. With the advantages of high enzyme to substrate ratio, efficient digestion and reusability, immobilized enzyme reactor (IMER) gradually takes the place of in-solution proteolysis. In addition, it eliminates the risk of sample contamination and can be online coupled to other separation and identification systems [5].

For IMER, enzymes could be trapped [6], cross-linked [7], covalently bonded [8] and physical adsorbed [9] into different matrices, including membrane, the inner wall of capillary or microchannel, monolithic material and particles (see Table 1). Among various matrices, monolithic materials are used more widely owing to its obvious advantages [10]. To date, the most typical monolithic materials are organic polymer and silica-based inorganic polymer. Their preparations, properties and applications have been investigated extensively [11,12]. Unfortunately, the problems of the swelling or shrinkage of organic monoliths and the complicated preparation procedures of silica-based monoliths restrict their developments. Consequently, the organic–inorganic hybrid monolith which can overcome these difficulties has attracted attention of researchers.

Besides having the advantages of organic monolith and inorganic-based monolith, the organic–inorganic hybrid monoliths have characters of better pH stability and less shrinkage [22]. Zhang's group prepared organic–inorganic hybrid monolith matrix of enzymatic reactor with tetraethoxysilane and 3-aminopropyltriethoxysilane as precursors, and then covalently immobilized trypsin through a bifunctional reagent, glutaraldehyde. This method maintained the activity of trypsin due to milder reaction condition compared with epoxide-modification [23]. This IMER combined with μ-RPLC-MS/MS achieved high-throughput proteome analysis and improved identification of low-abundance proteins [24,25]. After that, Zhang's group also used tetraethoxysilane and γ-Glycidoxypropyltrimethoxysilane as precursors and immobilized trypsin via metal chelation ($Cu^{2+}$) to prepare IMER with great enzymatic ability and renewability, which was applied to efficient digestion of rat liver extract [26].

Recently, nanoparticles showed great potential as excellent enzyme support owing to their characters of large surface area

*Abbreviations:* MALDI-TOF-MS, matrix assisted laser desorption ionization time of flight mass spectrometry; IMER, immobilized enzymatic reactor; i.d., inside diameter; o.d., outside diameter; BSA, bovine serum albumin; Cyt-C, cytochrome C; SEM, scanning electron microscopy; RSD, relative standard deviation

* Corresponding author. Tel.: +86 21 64253977; fax: +86 21 64233161.
*E-mail address:* zhanglingyi@ecust.edu.cn (L. Zhang).

[1] These two authors contributed equally.

0039-9140/$ - see front matter © 2013 Elsevier B.V. All rights reserved.
http://dx.doi.org/10.1016/j.talanta.2013.11.037

**Table 1**
The characteristics and applications of various immobilized materials.

| Carriers | Characteristics | Application |
|---|---|---|
| Membrane polyvinylidene fluoride membranes based reactor [13]; flat-sheet nylon membrane reactor [14] | Short radical diffusion distances; high localized enzyme concentration | Identification of low-abundance proteins in complex yeast cell lysates; efficient digestion even in presence of sodium dodecyl sulfate (SDS) |
| Inner wall of capillary or microchannel poly(ethylene-terephthalat)based reactor [15]; dextran-modified fused-silica capillaries reactor [16] | Good control of microfluidics; integration of many processes in one device | Integrated the reactor with the separation procedure and MS to analyze the sequence of protein samples extracted from liver cells; digested effectively of human hemoglobin |
| Monolithic material hydrophilic monolith based reactor [17]; porous polymer monolith based reactor [18] | Facile preparation; fast mass transfer; low backpressure; fine biological compatibility; easy modification | Identified successfully of *Escherichia coli* extract; applied to the digestion of different molecular weight and complexity such as human serum albumin, β-casein and ribonuclease B |
| Particles gold nanoparticles entrapped microreactor [19] and so on [20,21] | Large surface area; pore sizes tailored to protein molecule dimension; functionalized surface | Identified much proteins by the digestion or real proteins mixtures isolated from mouse macrophages; identified of digestion of human extract by the microreactor |

and some special surface properties [27]. Li et al. [28] fixed magnetic microspheres into capillary by magnetic force. Trypsin was immobilized by chelation with $Cu^{2+}$ modified on the surface of nanoparticles. Finally, the digestion efficiency of this reactor reached 21% and 77% for bovine serum albumin (BSA) and cytochrome C (Cyt-C) respectively, and 7 proteins of rat liver were identified. Min et al. [29] firstly introduced size-selective proteolysis based on the mesoporous silica trypsin nanoreactor. After trypsin was immobilized on thiol-modified SBA-15 particles, the nanoreactor was applied for digestion of a complex protein sample. The results showed that it digested low-molecular weight proteins preferentially while excluding high-molecular weight proteins. But applications of nanoparticle enzymatic reactors were limited by high back-pressure, nonuniform packing and difficult control of reactor aperture. In our previous work [30,31], the hybrid monolith columns were prepared by incorporating nanoparticles $Fe_3O_4$@$SiO_2$–$NH_2$ and SBA-15–$NH_2$ into monolithic materials and evaluated with mixture of organic acids in capillary electro-chromatography (CEC) mode. The selectivity and column efficiency were greatly enhanced by embedding of nanoparticles.

In this study, a novel hybrid matrix for enzymatic reactor was prepared by incorporating amino-modified SBA-15 nanoparticles into the hybrid organic–inorganic monolith, and covalently immobilizing trypsin through glutaraldehyde. The preparation and operation conditions including nanoparticles percentage and residence time were optimized. BSA, Cyt-C, myoglobin and rat liver extracts were used to evaluate the performance of the enzymatic reactor.

## 2. Materials and methods

### 2.1. Instruments and chemicals

The sample was pushed into reactor by a syringe pump (Baoding Longer Precision Pump Co., Ltd., China). Sol–gel solution and samples were mixed by a Vortex vibration (QL-901, Kylin–Bell Lab Instruments Co., Ltd., China). The nanoparticles were homogeneously dispersed in solution by an ultrasonic cleaner (AS3120, Tianjin Aote Saiensi Instrument Co., Ltd., China). The morphologies of the monolith and nanoparticles were observed by scanning electron microscope (SEM) of JSM-6360LV (JOEL, Japan). Fused-silica capillary with 100 μm i.d. and 365 μm o.d. was purchased from Sina Sumtech Co., Ltd. (Hebei, China). The temperature of digestion was controlled by the column oven (Dalian Elite Analytical Instruments Co., Ltd., China).

Tetraethoxysilane (TEOS, 98%), 3-amino-propyltriethoxysilane (APTES, 99%) and N-(3-(trimethoxysilyl)-propyl)-ethylenediamine (PEDA) were purchased from ACROS (Shanghai, China), which were used directly without further purification. Cetyltrimethyl ammonium bromide (CTAB) was purchased from Crystal Pure Reagent (Shanghai, China). Trypsin (bovine pancreas), Cyt-C (horse heart), myoglobin (horse skeletal muscle) and BSA (bovine serum) were obtained from Sigma-Aldrich (Milwaukee, WI, USA); rat liver was obtained from The Second Military Medical University.

### 2.2. Preparation and modification of nanoparticles

SBA-15 nanoparticles were prepared according to Ref. [32] (see Supplementary materials). Modification of SBA-15 nanoparticles with amino group was similar to Ref. [30]. Briefly, mixture of 7 mL methanol, 2 mL PEDA and 1 mL water were added into 10 mg SBA-15 nanoparticles followed by stirring for 24 h at room temperature (about 20 °C). The SBA-15–$NH_2$ nanoparticles were cleaned with methanol and water several times, and then put into oven of 60 °C overnight.

### 2.3. Preparation of hybrid organic–inorganic monolith

Fused silica capillary was pretreated according to Ref. [33]. The monolith preparation solution (MPS) containing 12 μL TEOS, 118 μL APTES, 215 μL ethanol, 32 μL water and 8 mg CTAB was mixed by vortex oscillator and ultrasonic apparatus in turn. After that, 100 μL MPS was added into 2.5 mg SBA-15–$NH_2$ nanoparticles, then the reaction solution was homogenized by vortex oscillator for 1 min at 0 °C and ultrasonic apparatus for 1 min in turn. After introducing the reaction solution into the capillary, the capillary was sealed by rubber and put into water bath of 40 °C for 24 h. Subsequently, the column was rinsed with ethanol, water and 100 mmol/L $NaH_2PO_4$ (pH=8.0) in turn to remove CTAB and other residuals of reactants. The synthetic steps of hybrid monolith containing nanoparticles were shown in Fig. 1A. The hybrid monolith without nanoparticles was also prepared for comparison using the method described elsewhere [24].

### 2.4. Preparation of enzymatic reactor with trypsin immobilized

The monolithic capillary column was rinsed with 10% (v/v) glutaraldehyde dissolved in 100 mmol/L phosphate buffer (pH=8.0) for 6 h at room temperature and then washed by 100 mmol/L phosphate buffer. After that, 2 mg/mL trypsin dissolved in 100 mmol/L phosphate buffer (pH=8.0) containing 50 mmol/L benzamidine and 5 mg/mL sodium cyanoborohydride ($NaCNBH_3$) was pushed into capillary continuously (0.2–0.8 μL/min) for 24 h at 4 °C to immobilize trypsin onto the hybrid support. Then nonspecifically absorbed trypsin was removed by pumping 20% acetonitrile (ACN) (v/v) in 100 mmol/L phosphate buffer for 4 h. And the residual aldehyde group on the surface of the support was deactivated by 1 mol/L Tris–HCl (pH=8.0) for 4 h. Finally, the enzymatic reactor was stored in 50 mmol/L Tris–HCl buffer (pH=7.5) containing 10 mmol/L

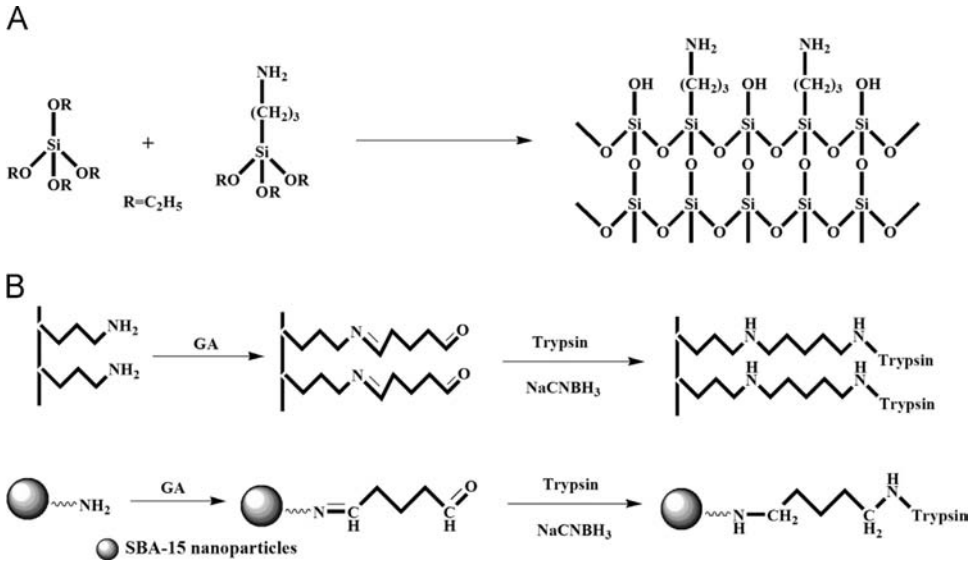


**Fig. 1.** Schemes of preparation of hybrid organic–inorganic monolith containing SBA-15 nanoparticles (A) and trypsin immobilization (B).

$CaCl_2$ and 0.02% $NaN_3$ (w/v) at 4 °C. The synthesis procedure was presented in Fig. 1B. The hybrid monolith without nanoparticles was also immobilized with trypsin as described elsewhere [24].

### 2.5. Sample preparation

The protein was dissolved in 50 mmol/L $NH_4HCO_3$ (pH=8) containing 8 mol/L urea and then reduced in 10 mmol/L dithicthreitol for 1 h at 56 °C, followed by alkylation in dark in 20 mmol/L iodoacetamide for 30 min at 37 °C after cooling to room temperature. The denatured sample was diluted by 50 mmol/L $NH_4HCO_3$ (pH=8) to intended concentration when using.

The on-column digestion (dynamic mode) was performed by injecting the denatured sample at a constant flow rate at 37 °C. The digestion products were collected and analyzed by MALDI-TOF-MS.

The in-solution digestion was carried out by putting trypsin into the denatured sample with an enzyme-to-substrate ratio of 1:50 (w/w). Subsequently the solution reacted at 37 °C for 12 h. At last, 2% (v/v) formic acid was added to end the reaction.

### 2.6. Extraction of rat liver

The rat liver was cleaned with cold saline (0.9% NaCl) to remove body fluid and some possible contaminants in blood, cut into small pieces. Then these small pieces were put into water containing 7 M urea, 2 M thiourea, 0.1% 3-[(3-cholamidopropyl) dimethylammonio]-1-propanesulfonate (CHAPS), 1% dithiothreitol (DTT), and 50 mM phenylmethylsulfonyl fluoride (PMSF) at ratio of 1:8 (g/mL) in an ice bath. Then it was homogenized for 30 min and centrifuged for 15 min at 12,000 g/min. The supernatant was collected and alkylated by iodoacetamide and stored at −20 °C for further analysis.

### 2.7. RPLC separation of rat liver extract

The RPLC separation experiments were performed on the Elite P1201 pumping system (Dalian Elite Analytical Instruments Co., Ltd., China) using column packed with SinoChrom ODS-BP particles (5 μm, 4.6 mm × 25 cm). Binary solvent composing of A (0.1% TFA in water, v/v) and B (0.1% TFA in ACN, v/v) was used as mobile phase. Gradient elution was set as follows: 0–30 min, linear gradient from 0% B to 20% B, 30–140 min, linear gradient from 20% B to 90% B; 140–160 min, 90% B. The flow rate was 1 mL/min and wavelength of UV detector was set at 215 nm. Chromatographic data acquisition and processing were performed by an EC2006 Chromatographic Workstation. Target fraction was collected and dried by $N_2$. The dried fraction was dissolved in 50 μL 50 mmol/L $NH_4HCO_3$ (pH=8.0) and digested by enzymatic reactor in dynamic mode.

### 2.8. Protein identification using MALDI-TOF-MS

Digestion products of proteins (0.5 μL) and 10 mg/mL cyano-4-hydroxycinnamic acid (CHCA) matrix solution dissolved in aqueous solution containing 50% (v/v) ACN and 0.1% (v/v) TFA were loaded to the target plate at ratio of 1:1. MALDI-TOF-MS experiments were performed in positive ion mode on a 4800 proteomics analyzer (Applied Biosystems). The UV laser was operated at a 200 Hz repetition rate with wavelength of 355 nm. The accelerated voltage was operated at 20 kV, and mass resolution was maximized at 2000 Da. Myoglobin digested by trypsin was used to calibrate the mass instrument in internal calibration mode.

The sequence coverage and number of matched peptides (by Mascot database) of protein were used to evaluate the performance of the reactor. Sequence coverage is the sum number of amino acids in matched peptides divided by the total sequence length of protein.

The data were searched using Mascot as engine (Matrix Science, London, UK) and Swissprot was used as database to identify standard protein based on peptide mass spectra. The identification of proteins from rat liver extract was performed by NCBI database.

## 3. Results and discussion

### 3.1. Morphologies of SBA-15–$NH_2$ nanoparticles and hybrid monolith

SEM image of SBA-15–$NH_2$ nanoparticles is shown in Fig. 2A, which indicates that the rod-like SBA-15–$NH_2$ nanoparticles have average length of 1.2 μm and diameter of 500 nm. Comparison of the SEM images of monolith without SBA-15–$NH_2$ nanoparticles (Fig. 2B) and monolith containing SBA-15–$NH_2$ nanoparticles (Fig. 2C) suggests that incorporation of SBA-15–$NH_2$ nanoparticles has little effect on the porous character of monolithic matrix.

The SEM image shows that monolith containing SBA-15–$NH_2$ nanoparticles has become more compact after immobilizing trypsin (Fig. 2D), because trypsin is a protein with high-molecular weight (Mw=24,000 Da) and will occupy a certain space after immobilization. In spite of it, porous structure of monolith still exists.

### 3.2. Effect of nanoparticles percentage on performance of enzymatic reactor

To determine effect of nanoparticles percentage on enzymatic reactor, 0, 0.5, 2.5, and 4.0 mg SBA-15 nanoparticles were added into 100 μL MPS, respectively. Consequently, nanoparticles percentages in the reaction solution were 0 mg/mL, 5 mg/mL, 25 mg/mL and 40 mg/mL. All enzymatic reactors prepared with different nanoparticles percentages accomplished digestion of 1 mg/mL BSA. The digestion results are shown in Table 2, which suggest that highest digestion efficiency was obtained when nanoparticles percentage was 25 mg/mL. With addition of nanoparticles, high specific surface area of nanoparticles helped loading more enzymes into monolithic matrix of reactor, which resulted in better digestion efficiency. Moreover, the enlargement of surface area [31] would also increase the chance of protein reacting with enzyme. Both of these two factors were good for protein identification.

To prove this, immobilized trypsin was dissociated from the support by NaOH solution at room temperature and amount of immobilized trypsin was measured by Braford assay [24] (see Fig. S-1 in Supplementary materials). The result indicated that 3.05 μg of trypsin was immobilized in a 1 cm length reactor with SBA-15 nanoparticles incorporated when nanoparticles percentage was 25 mg/mL, which was about 1.2 times higher than reactor prepared without nanoparticles (2.60 μg). When nanoparticles percentage was increased to 40 mg/mL, the amount of immobilized trypsin increased to 8.41 μg. However, redundant nanoparticles led to bad permeability of columns and lower digestion efficiency, because excess nanoparticles blocked the column and led to higher back pressure. Therefore, 25 mg/mL nanoparticles percentage was used to prepare enzymatic reactor in the following experiments.

### 3.3. Effect of sample loading mode

To characterize digestion rate of enzymatic reactor, dynamic and static modes were performed respectively using 1 mg/mL BSA as model sample. In dynamic mode, protein sample flowed through reactor at a constant flow rate of 0.5 μL/min at 37 °C. In this mode, the residence time of protein in reactor was about 19 s. On the contrary, static mode was performed by filling the reactor with sample solution and letting it stand at 37 °C for 5 min to ensure adequate reaction time. After that the digestion products were washed out by 50 mmol/L $NH_4HCO_3$ and collected for MALDI-TOF-MS identification. The products were also tested by SDS–PAGE and the absence of protein in digestion products suggested BSA was digested in both static and dynamic modes. The sequence coverage of 60% and 47% (see Table 3) for static and dynamic modes showed that proteolytic efficiency of static mode was higher than that of dynamic mode owing to longer reaction time.

Effect of flow rate in dynamic mode on digestion efficiency was determined too. When the flow rate increased from 0.5 μL/min to 1 μL/min, the sequence coverage was decreased to 31% for 1 mg/mL BSA. Because faster flow rate resulted in shorter reaction time in the reactor and the protein could not contact with trypsin in time before flowing out from reactor. But when decreasing flow rate from 0.5 μL/min to 0.3 μL/min, the sequence coverage was similar to that of 0.5 μL/min (see Table 3). This could be caused by instability of the syringe pump at low flow rate. Considering potential of coupling with MS or HPLC, dynamic mode was used in the following experiments.

### 3.4. Effect of protein concentration on performance of enzymatic reactor

To investigate the effect of protein concentration on performance of enzymatic reactor, BSA and myoglobin with different concentrations were digested by the reactor. From Table 4, it could be seen that 0.0001 mg/mL BSA and myoglobin were digested with sequence coverage of 12% (9 peptides matched) and 15% (2 peptides matched), respectively. The low values of number of

**Table 2**
Database searching results of BSA digested by enzymatic reactor prepared with various nanoparticles percentages[a].

| Nanoparticles percentage (mg/mL) | 0 | 5 | 25 | 40 |
|---|---|---|---|---|
| Peptide matched | 23 | 23 | 29 | 20 |
| Sequence coverage (%) | 37 | 38 | 50 | 35 |

[a] Digestion conditions: sample, 1 mg/mL BSA; enzymatic reactor, 100 μm i.d × 2 cm; 0.5 μL/min; 5 min; dynamic mode; 37 °C.

**Table 3**
Database searching results of BSA digested by enzymatic reactor in static mode and dynamic mode of different flow rate.

| Mode | Static | Dynamic | | |
|---|---|---|---|---|
| Flow rate (μL/min) | – | 0.3 | 0.5 | 1 |
| Matched peptides | 39 | 31 | 29 | 19 |
| Sequence coverage (%) | 60 | 51 | 50 | 31% |

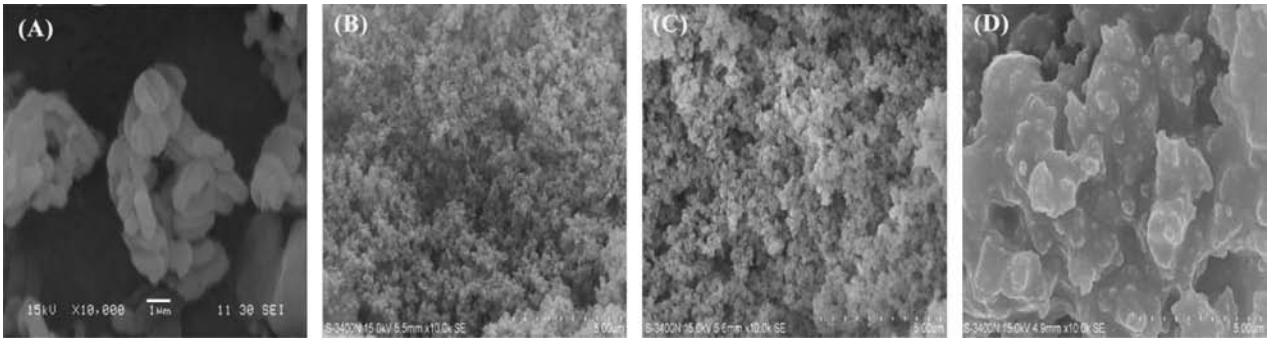


**Fig. 2.** SEM images of SBA-15–$NH_2$ nanoparticles (A), monolith without SBA-15–$NH_2$ nanoparticles (B), monolith containing SBA-15–$NH_2$ nanoparticles (C) and monolith containing SBA-15–$NH_2$ nanoparticles after immobilizing trypsin (D) at 10,000 × .

peptides matched and sequence coverage partly probably because that the protein concentration was close to the LOD of the detector. Despite the fact, they were obviously more effective than in-solution digestion. In addition, the higher digestion efficiency was achieved with increasing of sample concentration. Because BSA is a large globular protein (Mw=71,244 Da), the highest

**Table 4**
Database searching results of digestion products by enzymatic reactor in various sample concentration.

| | Reactor | | | | | In-solution |
|---|---|---|---|---|---|---|
| Protein concentration (mg/mL) | 0.0001 | 0.001 | 0.01 | 0.1 | 1 | 0.0001 |
| BSA | | | | | | |
| Peptides matched | 9 | 11 | 26 | 39 | 29 | 3 |
| Sequence coverage (%) | 12 | 11 | 41 | 65 | 50 | 4 |
| Myoglobin | | | | | | |
| Peptides matched | 4 | 9 | 9 | 12 | 16 | 1 |
| Sequence coverage (%) | 15 | 62 | 59 | 77 | 93 | 5 |

Digestion conditions see Table 2.

**Table 5**
Database searching results of digestion products by enzymatic reactors.

| Protein | Mw (Da) | Reactor containing SBA-15 nanoparticles | | | Reactor without SBA-15 nanoparticles | | | In solution | | |
|---|---|---|---|---|---|---|---|---|---|---|
| | | Matched peptides | Sequence coverage | | Matched peptides | Sequence coverage | | Matched peptides | Sequence coverage | |
| | | | Value (%) | SD[a] (%) | | Value (%) | SD (%) | | Value (%) | SD (%) |
| BSA | 71,244 | 29 | 50 | 3.1 | 23 | 37 | 2.5 | 22 | 36 | 2.1 |
| Myoglobin | 17,072 | 16 | 93 | 3.2 | 15 | 83 | 2.6 | 15 | 83 | 0.6 |
| Cyt-C | 11,810 | 11 | 71 | 2.6 | 11 | 63 | 2.5 | 8 | 54 | 1.7 |

Digestion conditions see Fig. 3.

[a] For all the standard deviation value: $n=3$.

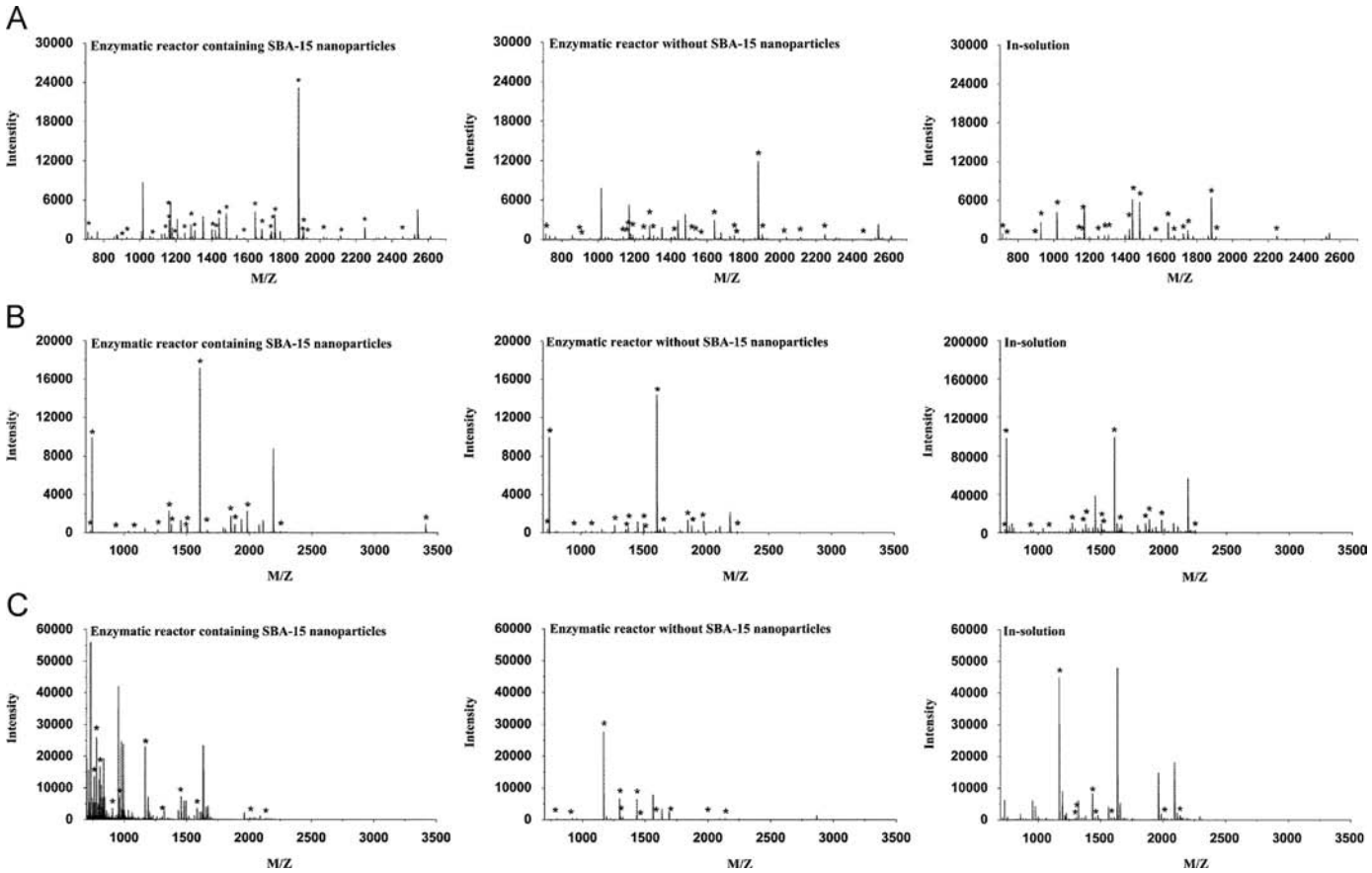


**Fig. 3.** Peptides mass fingerprinting of digestion products of BSA (A), myoglobin (B) and Cyt-C (C) using different digestion methods. Digestion conditions: protein, 1 mg/mL BSA, 1 mg/mL myoglobin and 1 mg/mL Cyt-C; enzymatic reactor, 100 μm i.d × 2 cm; flow rate, 0.5 μL/min in dynamic mode; digestion time, 5 min; temperature, 37 °C; in-solution digestion, enzyme/protein=1/50 (w/w), 12 h, 37 °C. "*" is assigned to matched peptide.

digestion efficiency was achieved when protein concentration was 0.1 mg/mL. Redundant protein might hinder reaction between BSA and trypsin and result in lower digestion efficiency. Considering no proteins were found in proteolytic products even for high concentration protein samples, which was confirmed by SDS-PAGE, the loss tryptic efficiency may come from incomplete digestion of some enzyme cutting sites. But for myoglobin, when the concentration increased to 1 mg/mL, sequence coverage of 93% (16 peptides matched) was obtained.

### 3.5. Reproducibility and stability of immobilized trypsin reactor

To study the reproducibility and stability of enzymatic reactor, 1 mg/mL BSA sample flowed through reactor about 5 min at 37 °C with flow rate of 0.5 μL/min. The relative standard deviation (RSD) values of digestion efficiency were 6.3% ($n=4$) for column-to-column analysis and 6.5% ($n=3$) for batch-to-batch analysis which showing good reproducibility. (see Table S-1 in Supplementary materials)

To test the stability of reactor, it was stored in 50 mmol/L Tris–HCl buffer containing 10 mmol/L $CaCl_2$ and 0.02% $NaN_3$ (pH=7.5) at 4 °C for 25 days. The sequence coverage was 43% (26 peptides matched) for 1 mg/mL BSA, which was comparable to the initial value of 50 % (29 peptides matched).

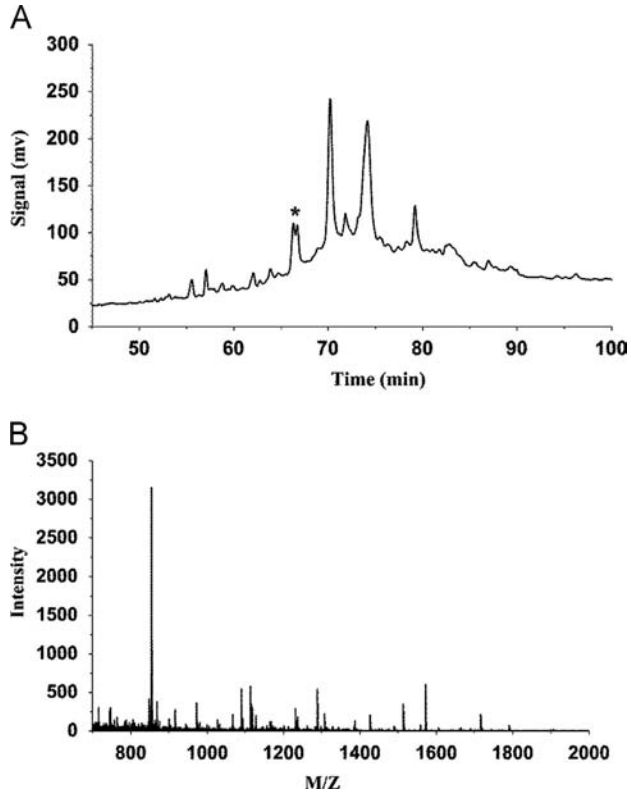


**Fig. 4.** Chromatograms for rat liver extract (A) and peptide mass fingerprinting of fractions labeled "*" (B). Separation conditions: mobile phase: A: 0.1% TFA in $H_2O$, 0.1% TFA in ACN; gradient conditions: 0% B(0 min)–20% B(30 min)–90% B(140 min)–90% B(160 min); injection volume: 200 μL; detection wavelength: 215 nm. Digestion conditions: sample, fraction labeled "*" of rat liver extract; enzymatic reactor, 100 μm i.d. × 5 cm; 0.5 μL/min; dynamic mode; 37 °C.

### 3.6. Digestion of standard proteins

Standard protein of BSA, myoglobin (Mw=17,072 Da) and Cyt-C (Mw=11,810 Da), which contain multiple cleavage sites, were chosen as model samples for digestion. Enzymatic reactor immobilized trypsin with a length of 2 cm was used. Samples were hydrolyzed in dynamic mode with the flow rate of 0.5 μL/min at 37 °C. At the same time, results of 12 h in-solution digestion and enzymatic reactor without SBA-15 nanoparticles digestion were also presented for comparison. Table 5 shows the results of database searching and corresponding peptides fingerprinting are shown in Fig. 3 (the details are presented in Table S-2 in Supplementary materials).

From Table 5, it can be seen that the sequence coverage were 50% (29 peptides matched) for BSA, 93% (16 peptides matched) for myoglobin and 71% (13 peptides matched) for Cyt-C, which were higher than in-solution digestion, although the residence time of protein in reactor was 1/2200 to in-solution digestion (19 s vs 12 h). Compared with the enzymatic reactor without SBA-15 nanoparticles, this reactor has higher digestion efficiency owing to the incorporation of SBA-15 nanoparticles. Moreover, in comparison with other IMERs with trypsin immobilized, for example, magnetic silica microspheres [28] based IMER whose sequence coverage of Cyt-C and BSA was 77% and 21% and poly (acrylamic-co-methylenebisacrylamide) monolith [7] based IMER whose sequence coverage of myoglobin and BSA were 79% and 58%, this enzymatic reactor shows good proteolysis ability for proteins with different molecular weights.

### 3.7. Application in digestion of one fraction from rat liver extract

To demonstrate the applicability of this enzymatic reactor in proteome analysis, the reactor (5 cm in length) was applied to digest one fraction collected in RPLC separation of rat liver (Fig.4) and then digestion products were analyzed by MALDI-TOF MS. Peptides peaks were observed from the peptides fingerprinting of the obtained digestion (Fig.4) which indicated the selected fraction (marked with "*" in Fig.4A) was digested by this enzymatic reactor. The search results showed that 11 unique proteins were identified with protein score more than 34 by performing against the NCBI database using the PMF method (Table 6).

**Table 6**
Proteins identified from labeled "*" fraction of the rat liver extract digestion by enzymatic reactor using MALDI-TOF MS.

| Identified protein | Accession no. | MW | Score |
|---|---|---|---|
| dynein heavy chain 9, axonemal [Rattus norvegicus] | gi\|392351290 | 516455 | 48 |
| rCG40442 [Rattus norvegicus] | gi\|149067944 | 7259 | 46 |
| 60S ribosomal protein L27a-like [Rattus norvegicus] | gi\|27720149 | 16653 | 39 |
| pelota homolog [Rattus norvegicus] | gi\|149059386 | 18514 | 37 |
| Dynein heavy chain9, axonemal isoform2 [Rattusnorvegicus] | gi\|293340174 | 516804 | 37 |
| rCG37815, isoform CRA_a [Rattus norvegicus] | gi\|149046719 | 47680 | 37 |
| osteoregulin-like protein [Rattus norvegicus] | gi\|22212816 | 47701 | 36 |
| transcription factor 15 [Rattus norvegicus] | gi\|270483807 | 20994 | 36 |
| nedd4 binding protein 3 [Rattus norvegicus] | gi\|76559919 | 60468 | 35 |
| protein Shroom1-like [Rattus norvegicus] | gi\|392331734 | 82979 | 35 |
| rCG34378, isoform CRA_k [Rattusnorvegicus] | gi\|149052057 | 13810 | 35 |

## 4. Conclusions

A hybrid organ–inorganic monolithic enzymatic reactor with SBA-15 nanoparticles incorporated was prepared for protein analysis. Due to the existence of SBA-15 nanoparticles, the hybrid monolith had larger specific surface area and were loaded more enzymes which led to an efficient digestion of proteins within a short time. Moreover, further research of bi/multiple enzyme reactor prepared by immobilizing different enzymes to nanoparticles and hybrid organic–inorganic monolith at the same time may help to improve the reliability of protein identification.

## Acknowledgment

We gratefully acknowledge the support of the Specialized Research Fund for the Doctoral Program of Higher Education of China (20100074110016), and the National Science Foundation for Young Scientists (No. 21105027).

## Appendix A. Supplementary materials

Supplementary materials associated with this article can be found in the online version at http://dx.doi.org/10.1016/j.talanta.2013.11.037.

## References

[1] B.T. Chait, Science 314 (2006) 65–66.
[2] J.-P. Lambert, M. Ethier, J.C. Smith, D. Figeys, Anal. Chem. 77 (2005) 3771–3788.
[3] J.R. Yates, C.I. Ruse, A. Nakorchevsky, Annu. Rev. Biomed. Eng. 11 (2009) 49–79.
[4] J.F. Ma, L.H Zhang, Z. Liang, Y.C. Shan, Y.K. Zhang, Trends Analyt. Chem. 30 (2011) 691–702.
[5] J.F. Ma, L.H. Zhang, Z. Liang, W.B. Zhang, Y.K. Zhang, Anal. Chim. Acta 632 (2009) 1–8.
[6] H.R. Luckarift, G.R. Johnson, J.C. Spain, J. Chromatogr. B Analyt. Technol. Biomed. Life Sci. 843 (2006) 310–316.
[7] S.B. Wu, L.L. Sun, J.F. Ma, K.G. Yang, Z. Liang, L.H. Zhang, Y.K. Zhang, Talanta 83 (2011) 1748–1753.
[8] S.K. Ozoner, B. Keskinler, E. Erhan, Mater. Sci. Eng. C Mater. Biol. Appl. 31 (2011) 663–668.
[9] S.B. Wu, L. Zhang, K.G. Yang, Z. Liang, L.H. Zhang, Y.K. Zhang, Anal. Bioanal. Chem. 402 (2012) 703–710.
[10] J. Krenkova, F. Svec, J. Sep. Sci. 32 (2009) 706–718.
[11] H.F. Zou, X.D. Huang, M.L. Ye, Q.Z. Luo, J. Chromatogr. A 954 (2002) 5–32.
[12] R.D. Arrua, C.I.A. Igarzabal, J. Sep. Sci. 34 (2011) 1974–1987.
[13] J.W. Cooper, C.S. Lee, Anal. Chem. 76 (2004) 2196–2202.
[14] F. Xu, W.H. Wang, Y.J. Tan, M.L. Bruening, Anal. Chem. 82 (2010) 10045–10051.
[15] Y. Liu, H.J. Lu, W. Zhong, P.Y. Song, J.L. Kong, P.Y. Yang, H.H. Girault, B.H. Liu, Anal. Chem. 78 (2006) 801–808.
[16] E.C.A. Stigter, G.J. de Jong, W.P. van Bennekom, Anal. Chim. Acta 619 (2008) 231–238.
[17] Y. Liang, D.Y. Tao, J.F. Ma, L.L. Sun, Z. Liang, L.H. Zhang, Y.K. Zhang, J. Chromatogr. A 1218 (2011) 2898–2905.
[18] E. Calleri, C. Temporini, F. Gasparrini, P. Simone, C. Villani, A. Ciogli, G. Massolini, J. Chromatogr. A, 1218, 8937–8945.
[19] Y. Liu, Y. Xue, J. Ji, X. Chen, J.L. Kong, P.Y. Yang, H.H. Girault, B.H. Liu, Mol. Cell Proteomics 6 (2007) 1428–1436.
[20] J.B. Kim, J.W. Grate, P. Wang, Trends Biotechnol. 26 (2008) 639–646.
[21] M.X. Gao, P. Zhang, G.F. Hong, X. Guan, G.Q. Yan, C.H. Deng, X.M. Zhang, J. Chromatogr. A 1216 (2009) 7472–7477.
[22] J.J. Ou, H. Lin, Z.B. Zhang, G. Huang, J. Dong, H.F. Zou, Electrophoresis 34 (2013) 126–140.
[23] S.B. Wu, J.F. Ma, K.G. Yang, J.X. Liu, Z. Liang, L.H. Zhang, Y.K. Zhang, Sci. China Life Sci. 54 (2011) 54–59.
[24] J.F. Ma, Z. Liang, X.Q. Qiao, Q.L. Deng, D.Y. Tao, L.H. Zhang, Y.K. Zhang, Anal. Chem. 80 (2008) 2949–2956.
[25] L.L. Sun, J.F. Ma, X.Q. Qiao, Y. Liang, G.J. Zhu, Y.C. Shan, Z. Liang, L.H. Zhang, Y.K. Zhang, Anal. Chem. 82 (2010) 2574–2579.
[26] J.F. Ma, C.Y. Hou, Y.L. Liang, T.T. Wang, Z. Liang, L.H. Zhang, Y.K. Zhang, Proteomics 11 (2011) 991–995.
[27] J. Kim, J.W. Grate, P. Wang, Chem. Eng. Sci. 61 (2006) 1017–1026.
[28] Y. Li, X.Q. Xu, B. Yan, C.H. Deng, W.J. Yu, P.Y. Yang, X.M. Zhang, J. Proteome. Res. 6 (2007) 2367–2375.
[29] Q.H. Min, R.A. Wu, L. Zhao, H.Q. Qin, M.L. Ye, J.J. Zhu, H.F. Zou, Chem. Commun. 46 (2010) 6144–6146.
[30] W. Lei, L.Y. Zhang, L. Wan, B.F. Shi, Y.Q. Wang, W.B. Zhang, J. Chromatogr. A 1239 (2012) 64–71.
[31] L. Wan, L.Y. Zhang, W. Lei, Y.X. Zhu, W.B. Zhang, Y.Q. Wang, Talanta 98 (2012) 277–281.
[32] Y.G. Wang, F.Y. Zhang, Y.Q. Wang, J.W. Ren, C.L. Li, X.H. Liu, Y. Guo, Y.L. Guo, G. Z. Lu, Mater. Chem. Phys. 115 (2009) 649–655.
[33] L.J. Yan, Q.H. Zhang, J. Zhang, L.Y. Zhang, T. Li, Y.Q. Feng, L.H. Zhang, W.B. Zhang, Y.K. Zhang, J. Chromatogr. A 1046 (2004) 255–261.